Emission spectra of high Rydberg states in a plasma: Stark-broadened neutral oxygen in the 7.5-μm region

Spiros Alexiou*
Department of Physics, Brown University, Providence, Rhode Island 02912

James C. Baird
Department of Physics and Department of Chemistry, Brown University, Providence, Rhode Island 02912
(Received 30 March 1990)

Plasma-broadened visible spectra have long been used to infer plasma parameters. In this work we examine the use of high Rydberg states in plasma spectroscopy for low-density plasmas. For low densities the high Rydberg states may be very useful because of their large widths and the fact that they are less susceptible to ion dynamical effects. We have calculated plasma-broadened spectra of the neutral oxygen $n=6\rightarrow n=5$ transition in the 7.5 μm region for a temperature around 10 000 K and electron densities $5\times10^{13}-10^{16}$ e/cm^3 and found that these spectra can be a useful probe for low-density plasmas. We also describe how selection rules can be used to greatly reduce the computational requirements.

I. INTRODUCTION

Pressure-broadened plasma spectra have long been used as plasma diagnostics. It has recently been suggested[1] that for low densities (up to say 10^{16} e/cm^3) plasma-broadened spectra of transitions between high Rydberg states, which will normally be in the infrared region (ir) for neutral emitters, may be promising as a diagnostic tool, because they are more sensitive (large widths) to the plasma parameters (primarily the electron density) and also because (in the case of emitters other than hydrogen) the relevant dipole matrix elements are much better known for the high Rydberg states that give rise to such transitions. In addition, optical thickness is not likely to be a problem for transitions between high-lying states. Also, for hydrogenic emitters ion dynamics is the main reason why quasistatic-dominated lines are preferred as density diagnostics to impact-dominated ones. Here ion dynamics will be less important, since the effective lifetime is shorter. Experimental work[2] on time-resolved infrared emission spectra of neutral oxygen in the 7.5-μm region confirms that large widths can occur for moderate densities. Besides the fact that the high Rydberg states involved are more polarizable (larger dipole matrix elements due to more extended wave functions), there are other factors contributing to the sensitivity of these lines, namely the Stark microfield is more effective in mixing the states because of the higher dipole matrix elements and the lower-energy separations between states of the same level. Also, more collisional channels that contribute significantly to the broadening are available. The total width of the line is further enhanced because of the many overlapping lines. The net result is that a rather small perturbation can have a large effect. Basically all these reasons have to do with the fact that each level separately is sensitive to perturbations. One could therefore also get a sensitive spectrum by considering transitions between a highly excited level and a low-lying level, for example, $n=6\rightarrow n=2$, which would be more sensitive and less susceptible to ion-dynamical effects than an n_α line, would be easier to model, and would normally be in the visible part of the spectrum. In some cases this may be a very good idea. However, the oscillator strength for such transitions will be very small, and the upper state will normally have very little population. This can raise questions about the observability of such lines, particularly if the plasma is not within the control of the experimenter. A further advantage of using lines in the ir region (rather than, say a high Balmer line) is that the width scales as λ^2. Oxygen was chosen in this work, not because it is in any sense better than say, hydrogen, but mainly because of the experimental work of Ref. 2. Our interest here is in low-density plasmas, both because the impact theory is a weak-coupling theory that breaks down more for the highly excited states we are considering for smaller densities than the absolutely maximum densities ($10^{18}-10^{19}$ e/cm^3) for which it is valid, and because at higher densities visible lines become sensitive too, so that there is no need to use high Rydberg states. Another region where the large widths associated with *ion* lines of transitions between high Rydberg states (which may still be visible) might be useful is that of high temperatures, where for transitions between low-lying levels Doppler broadening would normally dominate and thus it would be difficult to infer the electron density from the spectrum.

Because more states participate in the broadening of a given line, the computations are more involved and the matrix inversion [Eq. (3)] can be a problem, as it has to be performed $N_\omega\times N_E$ times, where N_ω is the number of ω points and N_E the number of electric microfields. Neither Mozer's[3] perturbation expansion nor assuming that Φ is spherically symmetric[4] are satisfactory ways of dealing with the inversion, so the matrix inversion is done rigorously, after the matrix is reduced to block diagonal

form. During the last few years very good line-shape computer programs have appeared, as described by Lee[5] and Woltz and Hooper.[6] Lee's code is impressively efficient, even for an upper state with very high principal quantum number, but he only calculates Lyman lines (his code has recently been extended so as to handle Balmer lines, too). He can then neglect lower-state interactions, and in any case he has a matrix of order n_u^2 to invert, where n_u is the principal quantum number of the upper state; because he is interested in Lyman lines, he is able to further simplify the problem by using m- and l-selection rules so that he only has two matrix inversions of dimensions n_u-1 and n_u-2, respectively, (24×24 and 23×23) at most, even for his largest n_u ($N_u=25$). Our matrices are of the order $n_u^2n_l^2$, where n_l is the principal quantum number of the lower level. Therefore we cannot neglect lower-state broadening, and thus our matrix inversion is much more of a problem. Woltz and Hooper have been able to reduce their matrix to block-diagonal form "at least in some approximations," but it is not clear how this is done. They have used the approximations of no lower-state broadening (and thus no interference terms) in their calculations, which are done for transitions between principal quantum numbers $n=4$ and $n=2$ and for $n=3$ and $n=2$. In this paper we show that even if we include *all* states of the upper and lower levels, in which case we have a matrix $n_u^2n_l^2$ to invert, this has a block-diagonal form and can be reduced to the inversion of two smaller matrices. This is basically an extension of Lee's m-selection rules. Furthermore, these smaller matrices are block tridiagonal.

II. THEORY

In the dipole approximation, the total power (summed over polarization and integrated over angles) is given by[4,7]

$$P(\omega)=\frac{4\omega^4}{3c^3}L(\omega)\ , \tag{1}$$

where $L(\omega)$ is the line shape:

$$L(\omega)=\sum_{i,f}\delta(\omega-\omega_{if})|\langle f|\mathbf{d}|i\rangle|^2\frac{e^{-H/kT}}{Z}\ , \tag{2}$$

with Z the partition function and H the total Hamiltonian.

In the impact approximation,[4,7] $L(\omega)$ is given by

$$L(\omega)=-\frac{1}{\pi}\frac{e^{-E_{\alpha'}/KT}}{Z}\int dE\ W(E)\mathrm{Re}\ \mathbf{d}_{\alpha'\beta'}\langle\alpha\beta|[i(\omega-\omega_{\alpha\beta})I+\Phi_{ab}]^{-1}|\alpha'\beta'\rangle\mathbf{d}^*_{\alpha\beta}\ . \tag{3}$$

α and α' are states of the initial level and β and β' states of the final level involved in the transition in question (in principle they are complete sets of states), Re denotes the real part, $W(E)$ is the ionic electric microfield distribution, whose calculation has attracted quite a bit of attention since the work of Baranger and Mozer,[8] I is the unit matrix, $\mathbf{d}$ is the dipole operator, and Φ is a collision operator with matrix elements[4,7]

$$\begin{aligned}\langle\alpha\beta|\Phi_{ab}|\alpha'\beta'\rangle=&-\frac{2\pi e^4n}{3(4\pi\hbar\epsilon_0)^2}\int_0^\infty f(v)vdv\int_{\rho_{\min}}^{\rho_{\max}}\rho d\rho\\
&\times\left[\int_{-\infty}^{\infty}dt_1\int_{-\infty}^{t_1}dt_2\frac{\rho^2+v^2t_1t_2}{(\rho^2+v^2t_1^2)^{3/2}(\rho^2+v^2t_2^2)^{3/2}}(e^{-i\omega_{\beta\beta''}t_2}\langle\beta|r_\mu|\beta''\rangle\langle\beta''|r_\mu|\beta'\rangle\right.\\
&\qquad+e^{i\omega_{\alpha\alpha''}t_1}e^{-i\omega_{\alpha'\alpha''}t_2}\langle\alpha|r_\mu|\alpha''\rangle\langle\alpha''|r_\mu|\alpha'\rangle)\\
&\left.-\int_{-\infty}^{\infty}dt_1\int_{-\infty}^{\infty}dt_2\frac{\rho^2+v^2t_1t_2}{(\rho^2+v^2t_1^2)^{3/2}(\rho^2+v^2t_2^2)^{3/2}}e^{i\omega_{\alpha\alpha'}t_1}e^{-i\omega_{\beta\beta'}t_2}\langle\alpha|r_\mu|\alpha'\rangle\langle\beta'|r_\mu|\beta\right]\ ,\end{aligned} \tag{4}$$

with n the density, $f(v)$ the Maxwell-Boltzman distribution, and with α'' and β'' denoting states of the upper and lower levels, respectively, (in this representation all states are eigenstates of the Stark Hamiltonian). One usually does the calculation in the unperturbed basis by letting $\alpha,\beta,\ldots$ denote unperturbed states and by changing Φ to $\Phi+i\mathbf{E}\cdot(\mathbf{d}_b^*-\mathbf{d}_a)/\hbar$. This was not done here for the purpose of keeping the code more general, as the unperturbed basis calculation is to first order in the Stark field and can only go up to second order (the same as Φ), while diagonalizing the Stark matrix can to up to all orders. Repeated indices μ, α'', and β'' are summed over. To this Φ, the Lorentz-Weisskopf strong collision estimate[7] was added. Since this estimate has been criticized[9] as overestimating the strong collisions, it was divided by 2 to bring it closer to Griem's[10] estimate. It was verified that the strong collision estimate is not critical and does not have an appreciable effect on the line shape for the densities we are considering. In the hydrogenic approximation, this gives a Φ operator of

$$\begin{aligned}\langle\alpha\beta|\Phi|\alpha'\beta'\rangle=&-\frac{4\pi ne^4}{3(4\pi\epsilon_0\hbar)^2}\left[\frac{2m}{\pi kT}\right]^{1/2}\left[\tfrac{1}{4}+\ln\frac{\rho_{\max}}{\rho_{\min}}\right]\\
&\times(\langle\alpha|r_\mu|\alpha''\rangle\langle\alpha''|r_\mu|\alpha'\rangle+\langle\beta|r_\mu|\beta''\rangle\langle\beta''|r_\mu|\beta'\rangle-2\langle\alpha|r_\mu|\alpha'\rangle\langle\beta'|r_\mu|\beta\rangle)\ ,\end{aligned} \tag{5}$$

with

$$\rho_{\min}=\max\left[\left[\frac{2}{3}\right]^{1/2}\frac{\hbar(n_i^2-n_f^2)}{mv},(n_i^2-n_f^2)a_0\right], \quad (6)$$

where a_0 is the Bohr radius and the upper cutoff is taken to be of the order of the Debye radius λ_D ($\rho_{\max}\approx 0.7\lambda_D$).

Of course one can use a G function[11] (basically a Green's function) in order to evaluate the electron electric-field–electric-field correlation function instead of our classical-path-based Φ. However, the differences are not significant until the frequency separation from the line center is close to the plasma frequency, and then the Lewis cutoff gives a very good approximation to the relaxation collision operators, as Smith[12] has shown. As far as the computer code is concerned, the main problem, the structure of the matrix that will be inverted, is dealt with here (assuming dipole interactions), and with efficient implementations of the G function[5] basically all one has to change is to substitute G for Φ. Note that the matrix structure is the same for neutral and ion emitters.

III. DETAILS OF THE CALCULATIONS

The necessary radial matrix elements were calculated from Chung *et al.*[13] and are in very good agreement (4% at worst) with hydrogenic calculations. $|\alpha\rangle,|\beta\rangle,\ldots$ are obtained as linear combinations of the unperturbed states in an lm representation when the Stark matrix is diagonalized. It was confirmed that the Stark effect significantly mixes only states having the same principal quantum number. The mixing coefficients with states with a different principal quantum number were less than 1% and were usually between 10^{-3} and 10^{-5} even for ion microfields that were substantially higher than the Holtzmark normal field. Hence the definition of a level as the set of states with the same quantum number is still valid (up to densities of 10^{18}–10^{19} e/cm^3) in our case, even though the s and p states do not mix with any other states and might be considered as different levels. The high Rydberg states with the same principal quantum number (except for $5f$ and $5g$ at the lowest density), however, are completely scrambled. The microfield distribution was calculated using Hooper's microfield program.[14] For our plasma parameters this microfield distribution is expected to be quite accurate, and more general microfield distributions such as the code APEX (Ref. 15) or density-functional microfields[16] are unnecessary; in fact, an APEX calculation shows no difference from Hooper's results. To avoid having to calculate the line shape for a very large number of electric fields, an integration rule with 15–20 adaptive Gaussian quadrature points was used (i.e., the integration region was divided into subregions which did not have the same number of points).

The transitions involved in the 7.5-μm line are level $n=6\rightarrow n=5$ at 7.448 μm (mainly $6f,g,h\rightarrow 5f,g$) and level $n=8\rightarrow n=6$ at 7.49 μm. Here, apart from the fact that the $8\rightarrow 6$ line is about 100 times less intense than the $6\rightarrow 5$ line and can thus be neglected, the two transitions are not overlapping in the sense that the levels $n=6$, 8, and 6, respectively, are not collisionally connected. In other words, the Φ matrix elements with, say, α in level 6, β in level 5, α' in level 8, and β' in level 5 or 6 are much smaller than the ones with α in level 6, β in level 5, α' in level 6, and β' in level 5, and thus the Φ matrix is to an excellent approximation block diagonal, with the two blocks in question corresponding to α in level 6, β in level 5, and α in level 8, β in level 6, respectively, and the blocks may therefore be inverted separately.

It is not enough to only consider states involved in the transitions, because collisional channels can add to the broadening. For example, the process: electron in level $n=6\rightarrow n=7$ (via a collision)$\rightarrow n=6$ (via another collision)$\rightarrow n=5$ (via spontaneous emission) contributes to the broadening. Normally, for low-lying levels such out-of-level collisional transitions (i.e., where n changes) are much less probable than collisional transitions between states of the same level and are thus neglected. In our case this is no longer true; for example, the radial integral $\langle n=6,l|r|n=7,l+1\rangle$ is about equal to $\langle n=6,l|r|n=6,l+1\rangle$ for the high-l states and can even be slightly larger. However, such collisions do not contribute very much to the broadening because the energy separations between states of different levels are larger, and this means that such an out-of-level collisionally induced transition occurs in a shorter time than the interlevel collision. Therefore, the radiation is interrupted for a shorter time, and this results in smaller widths. Mathematically, the imaginary exponentials in Φ, Eq. (4), oscillate very rapidly, and this results in smaller collision integrals. It was verified numerically that collision integrals for such out-of-level transitions are smaller than 10% of the interlevel collision integrals, and were neglected. Interlevel collision integrals, on the other hand, were found to be hydrogenic to a very good approximation and thus were evaluated analytically.

The matrix inversion implied in Eq. (3) is another problem, but can be done very efficiently if we exploit m-selection rules. Since we chose the z axis to coincide with the electric microfield, all Stark eigenstates $|\alpha\rangle,|\beta\rangle,\ldots$ are definite m states. This is all that is required for the following discussion. The m-selection rules thus imply

$$m_\alpha-m_{\alpha'}=m_\beta-m_{\beta'}=\begin{cases}1\\0\\-1\end{cases}. \quad (7)$$

The Φ matrix is labeled according to $m_\alpha m_\beta$ blocks. The $m_\alpha m_\beta$ block contains all combinations of states α and β with magnetic quantum numbers m_α and m_β, respectively. For example, row index 11 means α in block 1, β in block 1 (i.e., $m_\alpha=-5$, $m_\beta=-4$), index 12 means α in block 1, β in block 2 ($m_\alpha=-5$, $m_\beta=-3$), and so on. This is a block-banded matrix, with zeros between the diagonal and the outermost block of the band. We can put it in block-diagonal form by arranging the states in disjoint classes:

Class 1: $11,22,33,44,\ldots,N_bN_b$,
Class 2: $12,23,34,45,\ldots,(N_b+1)(N_b)$,
Class 3: $13,24,35,46,\ldots$,
...
Class N_b: $1N_b$,
Class N_b+1: $21,32,43,\ldots$,
Class N_b+2: $31,42,35,\ldots$,
...
Class N_b+N_a-1: N_a1, where $N_b=2l^b_{\max}+1=2n_l-1$ and $N_a=2l^a_{\max}+1=2n_u-1$, with the superscripts b and a denoting lower and upper levels, respectively. One may think of these classes as representing a constant $\Delta m=m_\alpha-m_\beta$. Because of the selection rule, Eq. (7), these classes are not connected and the matrix inversion is thus broken into N_b+N_a-1 inversions. This is basically the same diagonalization done by Vidal, Cooper and Smith.[17]

The reduction of the matrix inversion to the inversion of N_b+N_a-1 smaller matrices is a significant simplification, both for the speed of execution and storage. Note that this breaking up of the Φ matrix into blocks is possible even if the upper or lower "levels" consist of more than one n level. Furthermore, not all of these classes are needed, since the dipole product, $\mathbf{d}_{\beta\alpha}\cdot\mathbf{d}_{\alpha'\beta'}$ must also obey m-selection rules. Thus the first N_b classes $(11,\ldots,(1)(N_b))$ are all redundant except (in the case of n_α lines) the 11 class, and since any class can be specified by $m_\alpha-m_\beta$, there are only three classes that are of interest (corresponding to $m_\alpha-m_\beta=0,\pm1$). The $m_\alpha-m_\beta=\pm1$ classes contribute the same to the line shape, as can be easily verified, and this leaves us with two matrix inversions. Moreover, all classes have a band tridiagonal structure, because each $m_\alpha m_\beta$ block is only connected to itself and to its adjacent blocks (for example, the 33 block in class 11 is only connected to 22, 33, and 44). This fact is exploited to further cut down the execution time for the matrix inversion: a two-stage Gaussian elimination routine was implemented, where in the first stage row operations are performed to reduce the (current) diagonal block to a unit matrix, and in the second stage this unit matrix is used to eliminate the block below it until we are left with an upper triangular matrix, for which the same method is used (i.e., the current diagonal block is used to eliminate the block above it). The actual times for the code depend rather strongly on the specific computer used. For example, with a Convex computer (which does not do "loop collapse") the above procedure is not quite as fast as the highly optimized machine-language Convex veclib routines that take no advantage of the block tridiagonal structure.

Some additional simplifications arise from l-selection rules, in a variation of Lee's[5] method, and can be exploited using gather-scatter techniques, if we work in the unperturbed (field-independent) basis.

IV. VALIDITY OF THE QUASISTATIC APPROXIMATION

The effects of ion dynamics should also be addressed, since we are dealing with hydrogenic high Rydberg states and ion dynamics is known to be important for hydrogen lines at the densities considered here. Here ion dynamics is less important due to the large collision operator matrix elements. Griem[18] has investigated the validity of the quasistatic approximation in high-n $(n=90-170)n_\alpha$ lines in the radiofrequency range and has found that the ions as well as the electrons should be described by the impact approximation. Even though the temperature in his work is the same as here, the electron densities he was dealing with were extremely low (10^3 e/cm^3 at most), so this is hardly surprising.

Generally, speaking, ion dynamics will only be important for long times, i.e., near the line center. One way of checking the quasistatic approximation is to define an ion Weisskopf radius:

$$\rho^W_{\rm ion}=\sqrt{\tfrac{2}{3}}\frac{\hbar(n_i^2-n_f^2)}{mv_{\rm ion}}\approx 2.45\times10^{-7}\ \text{m} \tag{8}$$

for our transition and $T=10\,000$ K (m is the electron mass). The quasistatic approximation is assumed to hold if most ion collisions are strong, i.e., $\rho_{\rm mean}=(3/4\pi n)^{1/3}<\rho^W_{\rm ion}$, provided[19] that all strong collisions lead to static broadening. This is true if $\rho_{\rm mean}\ll\rho^W_{\rm ion}$, but there are also dynamic strong collisions ($\rho\approx\rho^W_{\rm ion}$). As Table I shows, ion-dynamic contributions are not expected to be a problem according to this criterion for $n\geq10^{15}$ e/cm^3. However, the 5×10^{13} and 5×10^{14}-e/cm^3 results are somewhat in doubt, according to this rough criterion.

Alternatively, we can use the more general condition[10,20] that, for the quasistatic approximation to hold, the typical ion-collision time must be much larger than the times that are important in the Fourier transform

$$\begin{aligned}L(\omega)&=\frac{1}{\pi}\text{Re}\int_0^\infty C(t)e^{-i\omega t}dt\\&=\frac{1}{\pi}\text{Re}\int^{0^\infty}dt\,\exp[t(\Phi-i\Delta\omega)]\ ,\end{aligned} \tag{9}$$

where $\Delta\omega=\omega-\omega_{\alpha\beta}$, that give us the line shape. The idea is that if the "lifetime," i.e., the "times of interruption of the spontaneous radiation" in Lorentz theory terminology, is much smaller than an ion-collision time, then ion dynamics may be neglected. This assumes that the lifetime cannot be longer than what is allowed by electron collisions alone, hence we compare the ionic collision time with the important times for the integration of $C(t)$ that gives the line shape. These important times are of the order of $\Delta\omega^{-1}$ in the wings, where $\Delta\omega$ is the separation from the line center and (for isolated lines) they are taken to be of the order of the width of the line in the

TABLE I. Ion dynamics (strong collision criterion).

Density (e/cm^3)	$\rho_{\rm mean}$ (10^{-7} m)
5.0×10^{13}	1.7
1.0×10^{14}	1.35
1.0×10^{15}	0.62
1.0×10^{16}	0.288

TABLE II. Ion-dynamic effects (important time criterion).

Density (e/cm^3)	τ_{ion}^{-1} (10^{10} Hz)	$\omega_{p,i}$ (10^{10} Hz)	Φ_{min} (10^{10} Hz)	Width (10^{10} Hz)
5.0×10^{13}	2.15	0.23	0.55	11.0
1.0×10^{14}	2.7	0.33	1.03	28.45
1.0×10^{15}	5.8	1.04	8.3	100
1.0×10^{16}	12.6	3.3	61.9	415

core. In our case, however, the width cannot be simply related to Φ, and the determination of these times requires diagonalizing the Φ matrix. This would be the rigorous way in all cases, but for isolated lines the width is of the same order of magnitude as the eigenvalues of Φ. In our case, with the hydrogenic approximation, Φ is a real symmetric matrix, and thus

$$e^{\Phi t}=Pe^{\Lambda t}P^{-1}\ , \tag{10}$$

where Λ is diagonal. The elements of Λ, the eigenvalues of Φ determine the "important times." The (absolutely) maximum and minimum eigenvalues may differ by an order of magnitude or so. They were determined for a microfield equal to about 1.5 times the Holtzmark normal field. It was numerically confirmed that they are very insensitive to the ionic microfield, as expected, since the eigenvalues of a matrix are independent of the representation used.

We can similarly check the validity of the impact approximation by comparing these times with a typical electron-collision time. Therefore if we denote by Φ_{min} and Φ_{max} the minimum and maximum eigenvalues of Φ, respectively, the following will certainly be *sufficient,* though not absolutely necessary validity criteria.

For the quasistatic approximation,

$$\Phi_{\text{min}}^{-1}\ll\frac{\rho_{\text{mean}}}{v_{\text{ion}}}\Longrightarrow\tau_{\text{ion}}^{-1}\ll\Phi_{\text{min}}\ , \tag{11}$$

and for the impact approximation,

$$\Phi_{\text{max}}^{-1}\gg\frac{\lambda_D}{v_{\text{el}}}\Longrightarrow\omega_{p,\text{el}}\gg\Phi_{\text{max}}\ , \tag{12}$$

where $\omega_{p,\text{el}}$ is the electron plasma frequency. It turns out that the width is of the order of the plasma frequency, so the Lewis cutoff was used.

The minimum important ion-collision time is of the order of τ_{ion}, the mean interionic radius over the ion velocity. A more typical ion-collision time is the inverse of the ion plasma frequency $\omega_{p,i}$. (The idea is that for a given $d\rho$ there is more phase space around the Debye radius λ_D, hence most collisions will be around λ_D.) Table II lists the inverses of these two times as well as Φ matrix elements and full width at half maximum (FWHM). The width is listed to show that Φ_{min} can be much smaller than the width, and thus application of the validity criterion of Ref. 20 to a case of many overlapping lines can lead to erroneous conclusions.

The conclusion is that ion dynamics is certainly not important for 10^{15} and 10^{16} e/cm^3 and even for 10^{14} e/cm^3 and 5×10^{13} no significant ion-dynamic effects are expected. It is true that for high Rydberg states one will have to start worrying about ion dynamics at lower densities than one would have to worry in the visible case. The reason is that Φ is larger for high Rydberg states; hence the minimum eigenvalue Φ_{min} will be larger than the Φ_{min} for low-lying states and thus would have a much better chance of being $\gg\tau_{\text{ion}}^{-1}$, where τ_{ion} is a typical ionic collision time.

V. RESULTS

Figures 1(a)–1(f) show model spectra for different plasma parameters. Also shown are the spectra evaluated at a microfield around the most probable one. The ω^4 factor from Eq. (1) as well as the Boltzmann factor were included. Doppler broadening is negligible in our case. It is clear that the spectra are completely impact dominated. One can obtain a fairly good approximation to the spectrum by evaluating it around the most probable microfield. The spectra are also rather insensitive to the temperature, but they are quite sensitive to the electron density. The sensitivity is not limited to the width: the entire line shape changes rather dramatically from a spectrum of essentially isolated lines (at our lowest density) to a broad feature. In particular, the asymmetry of the line [whose origin is clearly indicated by Fig. 1(a); the peak to the blue is due to transitions from upper levels that are a mixture of $6f$, g, h to $5f$, which does not mix at our lowest density] could be useful for inferring upper and lower bounds on the density without the need of a full calculation. Fits to Lorentzian and Gaussian line shapes show that for electron densities above 10^{15} e/cm^3 the line shape is rather well fitted by a Lorentzian. Gaussian fits are much worse. However, for the lower densities, Lorentzian fits are quite poor (as are Gaussian fits). The insensitivity to temperature is not usually expected for impact-dominated lines[21] and is one of the reasons why lines that are dominated by quasistatic broadening are usually preferred as density diagnostics. In our case the width is not simply related to Φ, and estimating the half-width from Φ can lead to serious errors. Figure 2 is a log-log plot of width versus electron density. The relationship between width and electron density is approximately linear (but with a slope quite different from Fig. 1) except for the line-merging region at the lower densities.

The main source of error in line-broadening calculations in cases where ion dynamics is not important and the dipole matrix elements are known quite accurately is

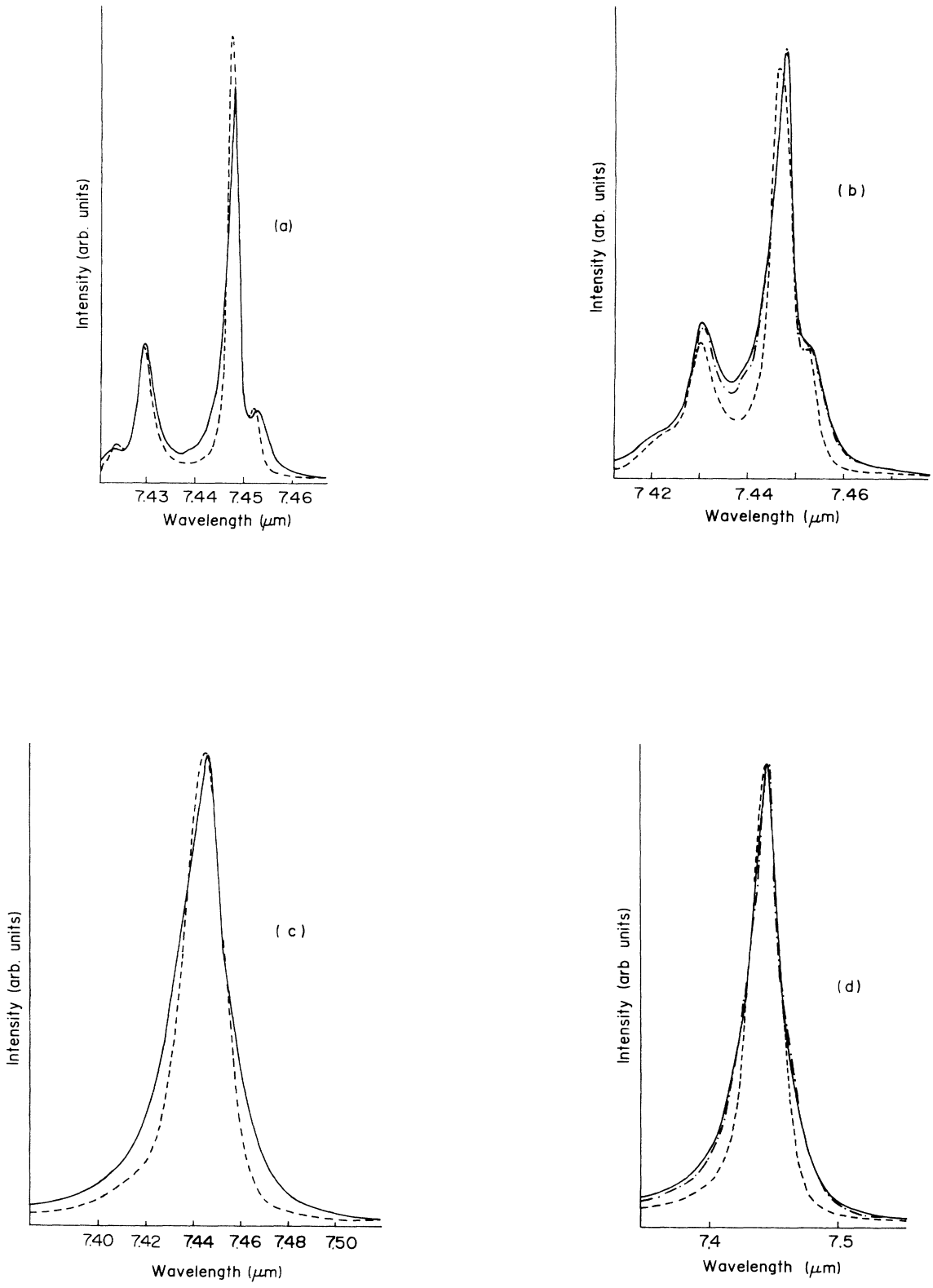

FIG. 1. Calculated spectra. Dashed line, $T=10\,000$ K, spectrum calculated at a microfield around the most probable one; solid line, $T=10\,000$ K, integrated over all microfields; dashed-dotted line [for (b), (d), and (f)], $T=15\,000$ K [for (b)] and $T=30\,000$ K [for (d) and (f)], integrated over all microfields. Electron density (e/cm^3): (a) 5×10^{13}, (b) 10^{14}, (c) 5×10^{14}, (d) 10^{15}, (e) 5×10^{15}, (f) 10^{16}. The spectra are scaled to the peak height of the solid line. For (d) and (f) the $T=15\,000$-K spectrum overlaps the $T=10\,000$-K integrated one.

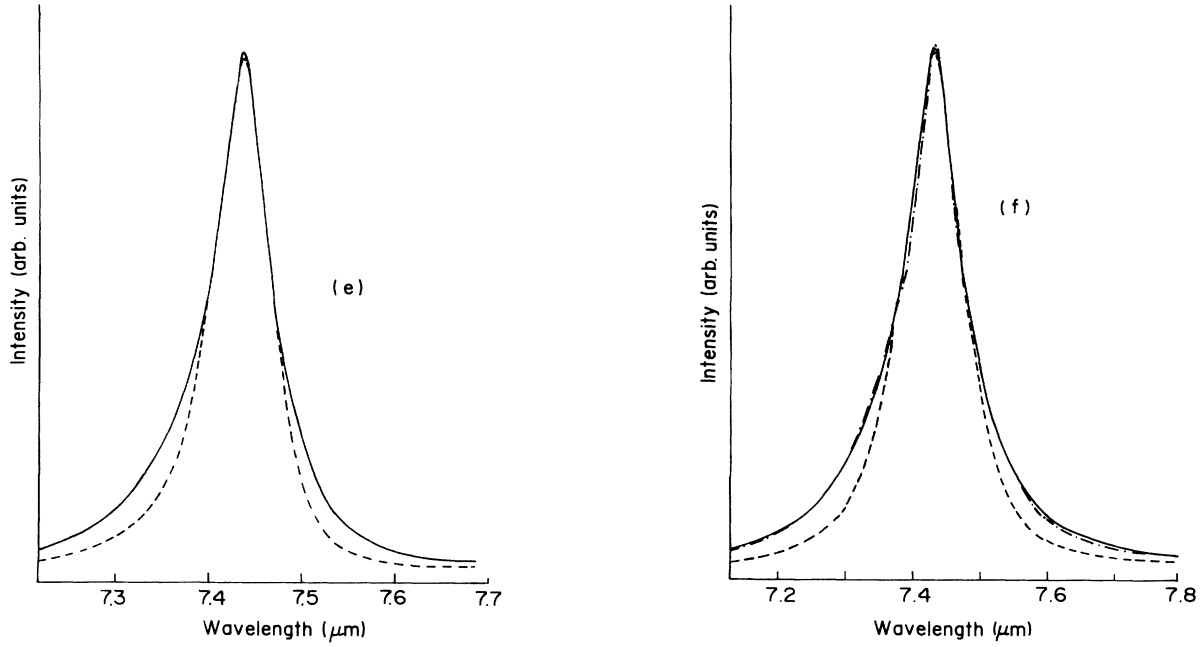

FIG. 1. (*Continued*).

thought to arise from the strong collision estimate, and this error will be more important at high densities. In our case, at our highest density, doubling the strong collision estimate made no change in the shape and increased the width by about 5%. Using a strong collision estimate of 0.1 made no change in the shape and also produced no discernible change in the width (less than 1%). Therefore a reasonable estimate of the uncertainty in the strong collision estimate is 4%. This is probably already too high. Additional sources of uncertainty are the use of the dipole interaction between emitter and perturbers and the no-quenching and hydrogenic approximations, and their combined effect could raise the uncertainty in the calculation to at most 8–10%. The present calculations should be of accuracy no worse than the standard (visible range) impact calculations, without the problems of ion dynamics.

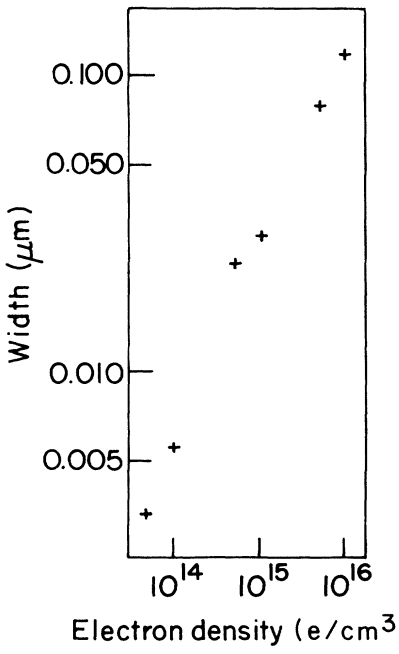

FIG. 2. Width (FWHM) vs electron density.

VI. CONCLUSIONS

The use of high Rydberg states in plasma spectroscopy has been investigated for the $n=6\rightarrow n=5$ transition in neutral oxygen. We have described how the computational problems can be dealt with, and have suggested that high Rydberg states can be a useful density diagnostic for low-density plasmas. Precision experiments in this region would be very helpful for accessing the diagnostic use of these high Rydberg states.

ACKNOWLEDGMENTS

The authors would like to thank Professor C. F. Hooper for the use of his microfield program. Computations were performed using the John Von Neuman Center (JVNC) supercomputers at Princeton, Grant No. CSC-13004 (PHY880942J). Some additional computations were done on the Convex at the Weizmann Institute. One of us (S.A.) would like to thank the people at JVNC for their hospitality during his stay there and Professor M. Baranger for useful discussions. In addition, S.A. would like to thank Y. Maron, A. Fruchtman, and the Plasma Physics group at Weizmann for their hospitality and H. Jarosch for his Gaussian and Lorentzian fitting routines. This project was partially supported by the U.S. Air Force Geophysics Laboratory in Hanscom, MA 01731, Contract No. 15105-WPR (AFGL F19628-83-C-0149).

*Present address: Department of Nuclear Physics, Weizmann Institute of Science, Rehovot 76100, Israel.

[1]J. C. Baird and S. Alexiou, Chem. Phys. Lett. **152**, 124 (1988).
[2]J. B. Lurie and J. C. Baird, Chem. Phys. Lett. **125**, 389 (1986).
[3]B. Mozer, Ph.D. thesis, Carnegie Institute of Technology, 1960.
[4]M. Baranger, in *Molecular and Atomic Processes,* edited by D. R. Bates (Academic, New York, 1962), Chap. 13.
[5]R. W. Lee, J. Quant. Spectrosc. Radiat. Transfer **40**, 561 (1988).
[6]L. A. Woltz and C. F. Hooper, Jr., Phys. Rev. A **38**, 4766 (1988).
[7]H. Griem, *Plasma Spectroscopy* (McGraw-Hill, New York, 1964).
[8]M. Baranger and B. Mozer, Phys. Rev. **115**, 521 (1959); B. Mozer and M. Baranger, *ibid.* **118**, 626 (1960).
[9]P. Kepple and H. R. Griem, Phys. Rev. **173**, 317 (1968).
[10]H. Griem, *Spectral Line Broadening in Plasmas* (Academic, New York, 1974).
[11]See, for example, J. Dufty, Phys. Rev. **187**, 305 (1969).
[12]E. W. Smith, Phys. Rev. **166**, 102 (1968).
[13]S. Chung, C. C. Lin, and E. T. P. Lee, J. Quant. Spectrosc. Radiat. Transfer **36**, 19 (1986).
[14]C. F. Hooper, Jr., Phys. Rev. **149**, 77 (1966); **165**, 215 (1968).
[15]C. Iglesias, J. Lebowitz, and D. MacGowan, Phys. Rev. A **28**, 1667 (1983).
[16]D. W. C. Dharma-wardana and F. Perrot, Phys. Rev. A **33**, 3303 (1986).
[17]C. R. Vidal, J. Cooper, and E. W. Smith, J. Quant. Spectrosc. Radiat. Transfer **11**, 263 (1971).
[18]H. R. Griem, Astrophys. J. **148**, 547 (1967).
[19]J. Seidel, in *Spectral Line Shapes,* edited by B. Wende (de Gruyter, Berlin, 1981).
[20]D. H. Oza, R. L. Greene, and D. E. Kelleher, Phys. Rev. A **37**, 531 (1988).
[21]G. Bekefi, C. Deutsch, and B. Ya'akobi, in *Principles of Laser Plasmas,* edited by G. Bekefi (Wiley, New York, 1976), Chap. 13.